J. Appl. Comput. Mech., 6(2) (2020) 248-258
DOI: 10.22055/JACM.2019.28827.1507

ISSN: 2383-4536
jacm.scu.ac.ir

M&MoCS

Shahid Chamran University of Ahvaz

Journal of Applied and Computational Mechanics

Research Paper

On the Influence of Riveting Process Parameters on Fatigue Life of Riveted Lap Joint

Pedram Zamani[1], Khalil Farhangdoost[2]

[1] Ph.D. Candidate, Department of Mechanical Engineering, Faculty of Engineering, Ferdowsi University of Mashhad
Azadi Square, Mashhad, 9177948974, Iran, Email: P.zamani@mail.um.ac.ir,

[2] Professor, Department of Mechanical Engineering, Faculty of Engineering, Ferdowsi University of Mashhad
Azadi Square, Mashhad, 9177948974, Iran, Email: Farhang@um.ac.ir

Received March 07 2019; Revised May 18 2019; Accepted for publication June 23 2019.
Corresponding author: Khalil Farhangdoost (Farhang@um.ac.ir)

Abstract. In this paper, influence of riveting process parameters, namely, riveting force, sheet thickness, friction coefficient and clearance fit are investigated on residual stress field and fatigue life of single riveted lap joint of AA2024 type. According to the effect of riveting induced residual stresses on fatigue life of riveted lap joint, these parameters are optimized to maximize the residual stress field. For this purpose, finite element simulations are performed for various combinations of the parameters according to Taguchi design of experiments. Afterwards, the parameter combination that maximize the residual stress field and the most effective parameters are obtained. The joint with maximum residual stress field is considered to have a semi-elliptical crack emanating from the rivet hole as an initial defect. Stress intensity factors are calculated by implementing two approaches: First, formulation overview that considers the effect of residual stress field, geometry and secondary bending, and second, the finite element method. The fatigue life of the joint is estimated using the obtained stress intensity factors and Paris-Erdogan rule. Finally, good accordance is found between results of these two approaches.

Keywords: Single lap joint, Residual stress, Stress intensity factor, Taguchi method, Fatigue life, Paris-Erdogan rule.

1. Introduction

Aircraft frames are complex structures that are composed by many subassemblies together. Riveting is considered as a suitable method for connecting elements of an aircraft fuselage. Besides, Lap joint is one of the most important ways of connecting the sheet metal parts. Riveted or bolted aircraft structures can be manufactured by either single or double lap joint. Failure in riveted joints can be catastrophic in aircraft industry. For example, the 1988 Aloha Airlines Flight 243 disaster, in which a portion of the passenger compartment disintegrated and resulted in one civilian casualty and several passengers sustained life threatening injuries, was attributed to a failure at and around one of the rivet holes, which propagated to the whole assembly [1]. Failure in riveted joints is affected by three main factors: stresses that are produced during riveting process, thermal fatigue, and vibration. Among these parameters, thermal fatigue and vibration are difficult to control [1]. So, controlling the stress field which is produced during the riveting process is very important. Consequently, it is suitable to control other factors that affect the joint's stress field such as riveting squeeze force, clearance fit, friction coefficient and sheet thickness.

Several researches have been performed on implementation of finite element method for riveted lap joints. Iyer et al. [2, 3] presented a numerical procedure based on finite element modeling. They examined the effect of countersinking the rivet head, its material, and friction between sheets. Their results revealed that all these factors were increased with

Published online: August 29 2019

severity of the countersink head. Szolwinski and Farris [4] analyzed the squeeze force effect on residual stress using a nonlinear 2-D FE model. These residual stresses are generally compressive near the rivet-hole interface and are tensile at the internal points far from the hole region. Moreira et al. [5] evaluated the residual stress intensity factor (SIF) for different crack dimensions and for various interferences both analytically and numerically. Rans [6] developed a simple finite element model in order to obtain residual stresses during the riveting process. Mathematical and mechanical models for elastic, plastic and spring-back deformation of the rivet was presented by Kaifu et al. [7]. Kafie-Martinez and Keating [8] simulated hot-driven riveting process. They obtained residual stress field which is induced due to riveting process and concluded that beneficial residual stress field decreases by increasing thickness of the substrate. In the following, Kafie-Martinez et al. [9] studied the stress distribution in a single riveted lap joint under the influence of various plate thicknesses. Result of their investigation revealed that the fatigue crack growth rate reduces in thinner plates.

In general, the presence of holes, rivet contact, residual stress, and geometric discontinuity means that the riveted joints play a key role in assessing the structural integrity of an aircraft fuselage. Some research works focused on geometrical and riveting process parameters of riveted joints through experimental study. Frost et al. [10] concluded that increasing the number of rows of rivet increases the fatigue strength of the joint. They also found the optimum spacing and position for the rivets array. Muller [11] studied the influence of squeeze force on the fatigue life of rivet using finite element method. He found that applying high squeeze force in riveting process could have a positive effect on fatigue life. The papers written by Fung and Smart [12, 13] provided evidence of a numerical parametric and fatigue study of riveted lap joints. Using both numerical and experimental methods, they investigated the effect of clearance fit, friction and clamping force on the fatigue life of the joint. Deng and Hutchinson [14] carried out an extensive FE analysis on simplified solid-rivet geometry in order to obtain the residual and clamping stresses. Trego [15] investigated the effect of compression residual stresses on the side of the rivet hole which showed that greater compression residual stress can improve fatigue life of the joint. Urban [16] provided an extensive summary of these works and carried out static and fatigue tests on different riveted joint configurations. He deduced that a detailed finite element (FE) model is required in order to obtain an accurate stress field with a view to establishing a good numerical/experimental correlation. Skorupa et al. [17] showed that riveting squeeze force and the rivet driven head dimensions are production variables that affect the quality of rivet installation and also fatigue performance of the joint. They observed same fatigue lives for round head and universal rivets. Riveted joint's static strength experiments and numerical studies on single and multi-row riveted lap joints were carried out by Pavan Kumar et al. [18]. Moslemi et al. [19] performed an experimental and finite element investigation to present a numerical approach to estimate fatigue life of single and double riveted coach peel joints by implementing finite element analysis and different fatigue life criteria. They found that Monson-Hirschberg criterion and experimental data have the best agreement in compare with SWT and Morrow.

It is significant to study the effect of riveting process parameters because of their influence on residual stress field and strength of the joint. This paper presents a finite element approach to determine the effect of various riveting process parameters, such as squeeze force, clearance fit, friction coefficient and sheet thickness, on the stress field and fatigue life. For this purpose, four values are considered for each parameter, finite element simulations are performed according to Taguchi design of experiments, and the optimum joint is achieved in order to maximize residual stress field. Accordingly, by assuming a semi-elliptical crack at the edge of rivet hole, two methods are considered for calculating stress intensity factors (SIFs). One of these methods, which is based on experimental formulations, considers the effect of residual stress around the hole, geometry and secondary bending. The other method implements finite element analysis to obtain SIFs. Afterwards, fatigue life of the joint is estimated using Paris-Erdogan rule. Additionally, good agreement is found between these two methods. In order to verify the FE solution, the experimental formula between rivet tail diameter and squeeze force is compared with such relation through FE solution.

2. Finite Element Modeling

2.1. Geometry and Material Properties

Due to the symmetry of the joint, only half of the joint was modeled (Fig. 1). Symmetric boundary conditions were applied to the center plane of the joint along the longitudinal direction. As shown in Fig. 1, boundary conditions of the joint were defined during riveting process as: displacement of the remote edges of sheet in y and z direction was set as zero, rivet head was restrained in y direction, and symmetry in z direction was defined as mentioned before.

The material of the rivet and sheet were defined as the isotropic plasticity model by considering rate effects. This material model uses power hardening rule, with the equation $\sigma = K\varepsilon^n$, where σ is true stress, ε is true strain, K is the strength hardening coefficient, and n is the strength hardening exponent. The material properties used in the simulations were selected from Rijck et al. [20] as shown in Table 1.

Table 1. Material properties.

	Young's modulus (GPa)	Poisson ratio	Yield strength (MPa)	Hardening parameter [20]	Paris-Erdogan power and coefficient
Rivet (2117-T4)	71.7	0.33	350	K=600MPa, n=0.3	$C = 1.1\times10^{-7}$, m=3.6
Sheets (2024-T4)	72.4	0.33	368	K=550 MPa, n=0.3	$C = 4.7\times10^{-7}$, m=3.7

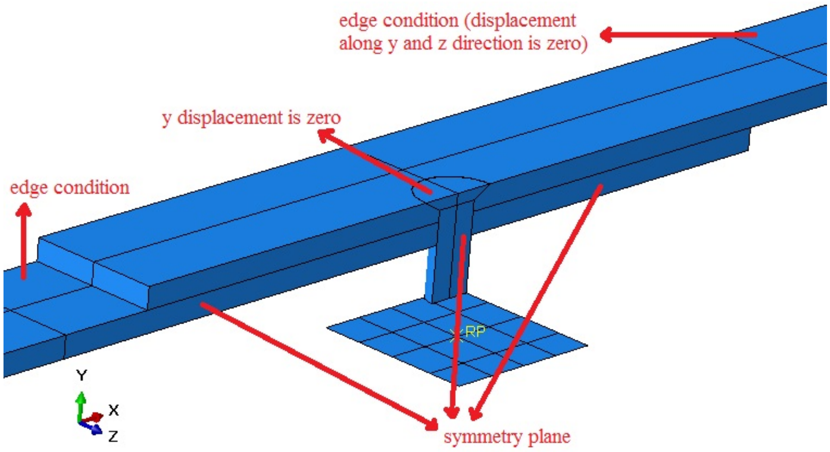

Fig. 1. Boundary conditions of a single riveted lap joint.

2.2. Model Definition

Three contact conditions were defined between surfaces: 1) surface interaction between hammer and rivet, 2) contact between rivet and sheets (rivet and lower sheet, rivet and surface of the hole), and 3) contact between two sheets. The surface interaction was selected as explicit surface to surface. Large deformations of the rivet shank during riveting process cause significant problem in converging the solution using implicit solver of the software. Moreover, the Abaqus Explicit/Dynamic analysis is an efficient solver for defining general contact conditions and uses large-deformation theory to carry out the models that experience large deformations. Hence, the solution type was defined as Dynamic/Explicit in order to achieve convergence in finite element analysis. The initial increment size and minimum increment size was selected as 0.1 and 1e-5, respectively. A constant force was applied to the rigid body in order to deform the rivet's leg and form the riveted joint (named as loading phase). The time of loading phase was considered to be 0.5 second during explicit/dynamic step and it was defined to have a ramp shape until it reach to the final value at the end of the step. Then, the force was defined as zero in the second step (unloading phase) and the rigid body has moved back. Three dimensional axisymmetric eight node standard elements with reduced integration were defined. The element distortion occurs due to large plastic deformation of the rivet during riveting process. Besides, element distortion is a computationally time-consuming issue and can stop the simulation. Thus, adaptive meshing was used to minimize distortion of elements and distortion control option was also activated. It is worth noting that in order to reach more concise results, mesh refinement was performed for stress field around the edge of the hole and the minimum element size after which a divergence happened, was selected. A typical mesh of axisymmetric model is shown in Fig. 2. Additionally, semi-elliptical cracks, which are introduced in next sections, were defined as seam and stress intensity factors were obtained using contour integral method and linear elastic fracture mechanics approach.

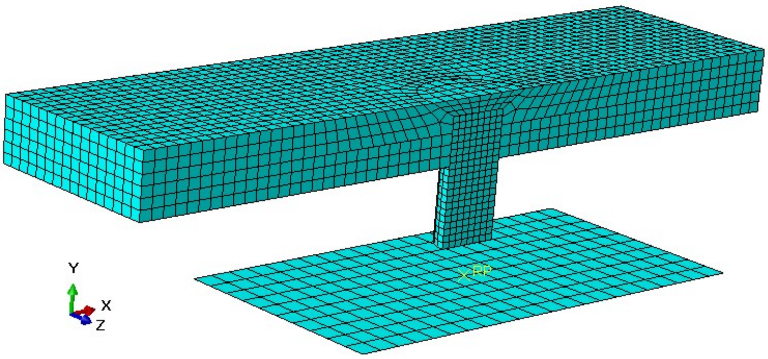

Fig. 2. A meshed instance of the single riveted lap joint.

3. Numerical Approach to Estimate Fatigue Life

Riveting process parameters such as riveting squeeze force, sheet thickness, clearance fit and friction coefficient directly affect the residual stress field around the rivet hole. Therefore, it is important to study the influence of these parameters on residual stress field. In this section, first, Taguchi design of experiments (DOE) was performed to investigate the influence of various parameters on residual stress field. It should be noted that higher compressive residual stress field improves fatigue life of the joint because this compressive stress field delays the crack growth. Therefore, the goal of Taguchi optimization procedure was considered to maximize residual stress field. Second, optimized residual stress field results were used in fatigue life estimation in combination with fracture mechanics approach.

3.1. Basics of Design of Experiments

It is noteworthy that Taguchi method provides two main results. Firstly, it shows which level of each parameter causes maximum residual stress. Secondly, it reveals the parameter that has the most effect on residual stress field among others. In this research, four parameters were considered and four levels were chosen for each parameter. As it is time consuming to study the effect of multi-level factors in a system, it is necessary to consider all possible conditions. Consequently, Taguchi's L16 orthogonal table was applied for designing experiments. This table decreases 256 possible experiments to 16 ones. Four factors with their corresponding levels are presented in Table 2 and design of experiments for these parameters is shown in Table 3.

As it is previously stated, the more increase in the residual stress field due to riveting process, leads to postponement in crack initiation and longer fatigue life. The approach to discuss the results of Taguchi orthogonal arrays is explained here. At first, the loss function should be calculated according to the goal of optimization procedure (higher-is-better) (Eq. 1).

$$L = \frac{1}{n}\sum\left(\frac{1}{y_i}\right)^2 \tag{1}$$

where n is the try number for each experiment, i is the number of experiment, and y is the maximum residual stress (goal function). Secondly, the signal to noise ratio is obtained according to the following equation [21]:

$$SN = -10\log(L_i) \tag{2}$$

where L is the loss function and i is the number of experiment. Subsequently, mean of signal to noise ratio for each factor was calculated at each level. After discussing on these mean values, the levels of each parameter at which the maximum residual stress field obtains, was achieved.

Table 2. Four factors and their corresponding levels.

Factor	Friction coefficient	Clearance fit	Riveting squeeze force	Sheet thickness
Level 1	0.2	0	7	2
Level 2	0.4	0.05	10	2.2
Level 3	0.6	0.1	13	2.4
Level 4	0.8	0.2	16	2.6

Table 3. Taguchi's orthogonal array for design of experiments.

Factor / Number of experiment	Friction coefficient	Clearance fit	Riveting squeeze force	Sheet thickness
1	0.2	0	7	2
2	0.2	0.05	10	2.2
3	0.2	0.1	13	2.4
4	0.2	0.2	16	2.6
5	0.4	0	10	2.4
6	0.4	0.05	7	2.6
7	0.4	0.1	16	2
8	0.4	0.2	13	2.2
9	0.6	0	13	2.6
10	0.6	0.05	16	2.4
11	0.6	0.1	7	2.2
12	0.6	0.2	10	2
13	0.8	0	16	2.2
14	0.8	0.05	13	2
15	0.8	0.1	13	2.6
16	0.8	0.2	7	2.4

3.2. Fatigue Life Estimation

3.2.1 Overview of fatigue life approaches

Fracture mechanics approach considers the second region of crack growth rate diagram in estimating fatigue life for a pre-defined crack. This region shows essentially a linear log-log relationship between crack growth rate (da/dN) and SIF range (ΔK) [22]. Where ΔK is defined as the difference between maximum and minimum SIFs during fatigue loading. This linear relationship was suggested by Paris and Erdogan [23] as follows:

$$\frac{da}{dN} = C\left(\Delta K\right)^m \tag{3}$$

where m and C are power and coefficient of Paris-Erdogan relationship, respectively. Thus, fatigue life can be calculated by integrating Eq. (3). Thereby, the most important part in computation of fatigue life is calculating accurate amounts of stress intensity factors. SIF calculation can be performed in two ways: (1) calculation of SIF by considering relationships from previous research works for cracks that emanate from hole. These relationships are based on experimental and numerical studies and consider the effect of geometry, residual stress field, and secondary bending, (2) calculation of SIF using finite element method.

The first method includes three main stages. Firstly, calculation of stress intensity factors according to geometry of crack. Secondly, calculation of stress intensity factors corresponding to residual stress effect around the rivet hole. Thirdly, calculation of stress intensity factors corresponding to secondary bending effect. Finally, the equivalent SIF is calculated by considering abovementioned stages and fatigue life is estimated. In second method, a finite element analysis is carried out using ABAQUS 6.11 to calculate SIFs and fatigue life of the riveted joint is estimated by implementing Paris-Erdogan rule.

3.2.2. SIF calculation using the experimental formulation for a semi-elliptical crack

Schijve et al. [24] carried out a couple of experimental tests and presented an experimental correction coefficient for stress intensity factor (Eq. (4)). Eq. (4) considers the effect of loading, width, hole and crack length in calculation of stress intensity factor. The crack was considered to be semi-elliptical through thickness crack that was initiated from the hole. Besides, the SIF at crack opening mode (K_I) can be calculated by Eq. (5).

$$\beta = \left[\frac{1}{0.539 + 1.93\frac{a}{R} + 2\left(\frac{a}{R}\right)^2} + \frac{\lambda+2}{2}\right]\sqrt{\frac{\lambda+1}{2}}\left[1 + \frac{a}{R}\frac{\lambda^3}{5}\right] \tag{4}$$

$$K_I = \beta\sigma\sqrt{\pi a} \tag{5}$$

In above equations, σ , a, and R represent far field stress, crack length and radius of hole, respectively. λ is defined as:

$$\lambda = \frac{1}{1 + \frac{a}{R}} \tag{6}$$

Beuth and Hutchinson presented a relationship for cracks emerging from a rivet hole where there is a pre-existing residual stress field due to the riveting process (Eq. (7)) [25].

$$\frac{K}{\sigma_R\sqrt{R}} = \sqrt{\pi\frac{a}{R}}G\left(\frac{a}{R}\right) \tag{7}$$

where a, R, σ_R and $G(a/R)$ are crack length, radius of hole, radial stress and a function that is defined by Beuth and Hutchinson. Beuth and Hutchinson stated that a reasonable estimate for σ_R should fall between half of the yield strength of the sheet and yield strength of the sheet material [25]. Additionally, after simulating the riveting process, maximum radial stress was achieved as 185 MPa.

Secondary bending is one of the most important factors that affects stress intensity factor. Calculation of secondary bending stresses is based on advanced beams theory. Rijck et al. used neutral line model to calculate stresses in a simple lap joint due to secondary bending effect. They finally presented Eq. (8) as secondary bending coefficient [26].

$$K_b = \frac{3}{1 + 2\sqrt{2}\tanh(\alpha L)} \tag{8}$$

where L is shown in Fig. 3 and α is defined as:

$$\alpha = \sqrt{\frac{3\sigma}{2t^2 E}} \tag{9}$$

σ , t and E stand for stress, sheet thickness and module of elasticity, respectively. Eq. (8) implies that the effect of the length of specimen on the secondary bending can be ignored.

According to abovementioned explanations, Table 6 shows stress intensity factors due to each factor. Then, equivalent stress intensity factor for each crack length was calculated by summing three SIFs.

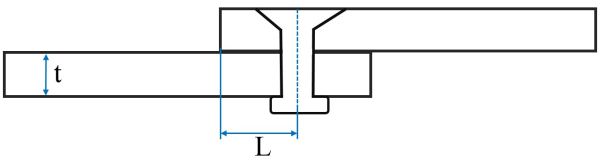

Fig. 3. Schematic of secondary bending parameters.

4. Results and Discussion

4.1. Results of Taguchi Analysis

Finite element modeling was performed for each experiment (Table 3) and the results in terms of maximum residual stress are stated in Table 4. As a typical result, residual stress state of 10th experiment is shown in Fig. 4. In continue, loss function was defined in a higher-better condition, because the higher residual stress field results in better fatigue life. In other words, higher-better condition belongs to the situation in which higher value of goal function is appropriate. So, the value of loss function and signal to noise ratio were calculated for each experiment and are shown in Table 4. Moreover, mean of signal to noise ratio for each factor was calculated for each level. For example, mean of SN ratios were calculated for the first factor (Riveting squeeze force) and in its first level. This calculation corresponds to mean of signal to noise ratio for the first level of riveting squeeze force. Mean of SN ratio for other factors and their corresponding levels were calculated using such the same way as mentioned (Table 5). Δ in Table 5 is defined as the difference between maximum and minimum values of mean SN ratio for each factor among its different levels. The factor that has the maximum value of Δ, has the most effect among other factors on the residual stress field. The most and least values of Δ belong to riveting squeeze force and clearance fit, respectively. It means that variations in riveting squeeze force affect the most on residual stress field in compare with the same variation in other factors. Priority of factors is introduced as rank numbers in Table 5. Variations in the lower rank number has more effect on residual stress field.

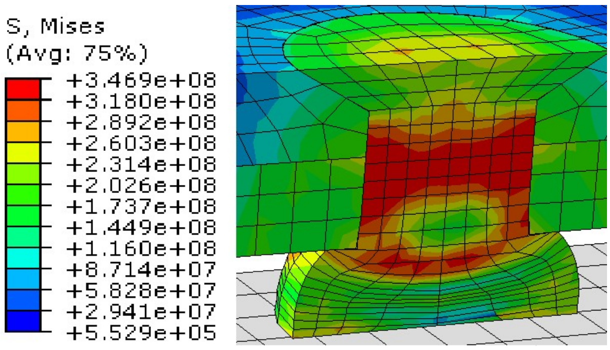

Fig. 4. Residual stress field in the 10th experiment (in Pa).

Table 4. Maximum residual stress, loss function and signal to noise ratio for each experiment.

Number of experiment	Maximum residual stress (MPa)	Loss function	Signal to noise ratio (SN)
1	341.4	8.5797	50.6653
2	348	8.2574	50.8316
3	344.8	8.4113	50.7514
4	343.9	8.4554	50.7287
5	342.3	8.5347	50.6881
6	333.8	8.9749	50.4697
7	349.6	8.1820	50.8714
8	347.4	8.2859	50.8166
9	348.1	8.2526	50.8341
10	346.9	8.3435	50.7865
11	342.5	8.5247	50.6932
12	348	8.2574	50.8316
13	347.4	8.2859	50.8166
14	344	8.4505	50.7412
15	343.3	8.4850	50.7135
16	340.5	8.6251	50.6424

Table 5. Mean of signal to noise ratio and rank number for each factor.

Factor	Friction coefficient	Clearance fit	Riveting squeeze force	Sheet thickness
Level 1	50.7443	50.7510	50.6176	50.7774
Level 2	50.7114	50.7073	50.7662	50.7895
Level 3	50.7863	50.7574	50.7858	50.7171
Level 4	50.7284	50.7726	50.8008	50.6865
Δ	0.0749	0.0653	0.1832	0.1030
Rank	3	4	1	2

Mean values of SN ratio, evaluated for each factor and according to different levels, are shown in Fig. 5. As it is shown in this figure, maximum value of Δ belongs to riveting squeeze force. However, maximum value of Mean SN ratio could be observed for each factor in different levels (Fig. 5). Maximum value of mean for riveting squeeze force was occurred in its last level. The maximum mean values of SN ratio for friction coefficient, clearance fit and sheet thickness were in their third, fourth and second levels, respectively. The mentioned levels are defined as optimum levels which can be used in design and fatigue analysis. It must be pointed out that the usage of these optimum values in a typical joint configuration could maximize the residual stress field. Additionally, according to trend of each factor in its levels, it could be inferred that increasing riveting squeeze force improves the residual stress field and higher sheet thicknesses lowers the residual stress. Therefore, although the increase in riveting force leads to increase in residual stress field and fatigue life in metallic joints, the opposite result is shown in metal-to-composite riveted joint fabricated by electromagnetic riveting process [27]. In order to verify the optimum factors (optimum joint), a 3D simulation of riveting process was conducted due to optimum levels of each factor. Then, result of this simulation was obtained and corresponding SN ratio was calculated. In continue, the error between the optimum SN ratio and other SN ratios was calculated. The comparison has shown a mean error of 4.82% between SN ratio for optimum joint and other experiments.

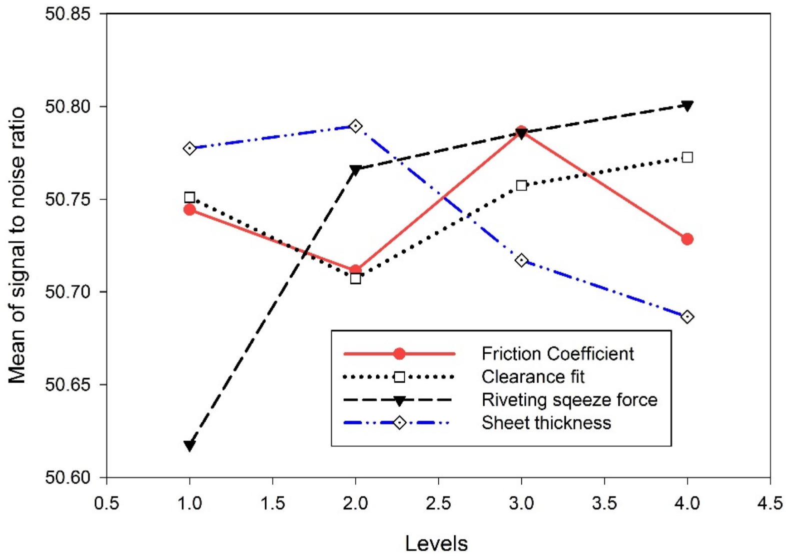

Fig. 5. Variations in Mean of SN ratio for different factors in four levels.

4.2. SIF results using finite element analysis

Fatigue life calculation of the riveted joint can be carried out using either linear elastic fracture mechanics (LEFM). In LEFM, local stresses in the vicinity of crack tip are solved according to elasticity theory. Therefore, study of crack and fatigue crack growth was accomplished through computation of SIFs. This approach is valid until the time that the plastic zone in the vicinity of crack (plastic radius) can be ignored in compare with the length of crack. In this paper, an emanating linear semi elliptical crack was considered as initial defect that is a common defect in different plates and structures containing a hole [28].

In order to obtain SIFs, first of all, the riveting process was simulated with a 16 kN riveting force, 2.2 mm sheet thickness, friction coefficient of 0.6 and a 0.2 mm clearance fit (known as optimum joint values). Then, an elliptical crack emanating from the sheet's hole was defined as it is shown in Fig. 6

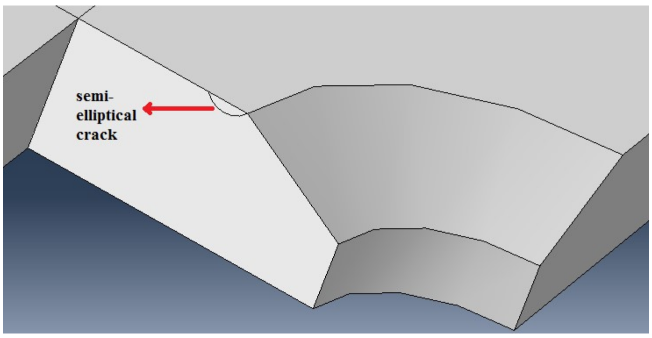

Fig. 6. Semi-elliptical crack emanating from sheet's hole.

The step of solution was defined as Dynamic/Explicit in finite element software. Maximum applied cyclic stress is 30 MPa and the load ratio was considered as zero. The SIFs were computed for different crack lengths. For each crack, contour integral method for calculating the SIFs was considered to have 10 integral contours, and after submitting the output results, the maximum value among these contours was considered as the SIF value. Fig. 7 shows a comparison between Newman's SIFs and FEM results for different crack lengths. This figure shows a mean error of 4% between FEM results and experimental formula. In continue, fatigue life of the riveted joint was calculated using Paris model for each crack length. Fatigue life estimations of abovementioned methods is shown in Fig. 8

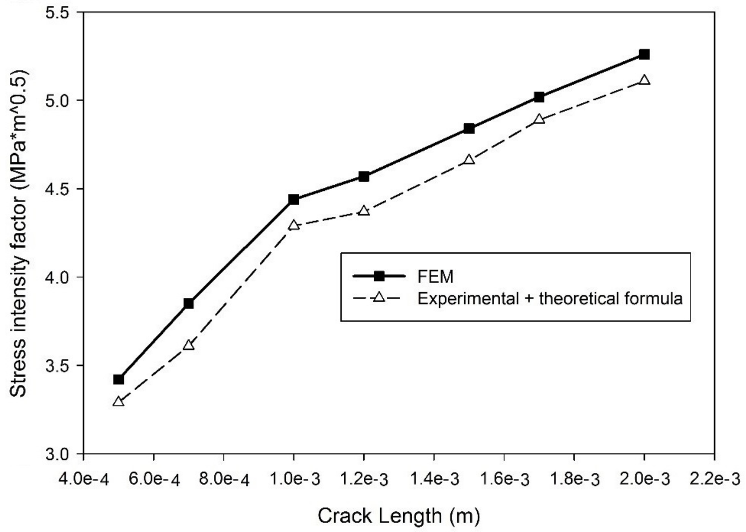

Fig. 7. Stress intensity factors resulted from FEM and experimental formula.

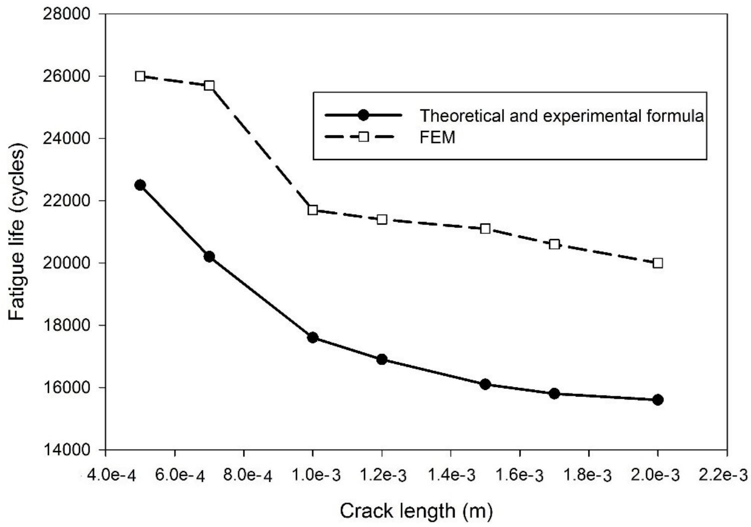

Fig. 8. Fatigue life variation according to different crack length.

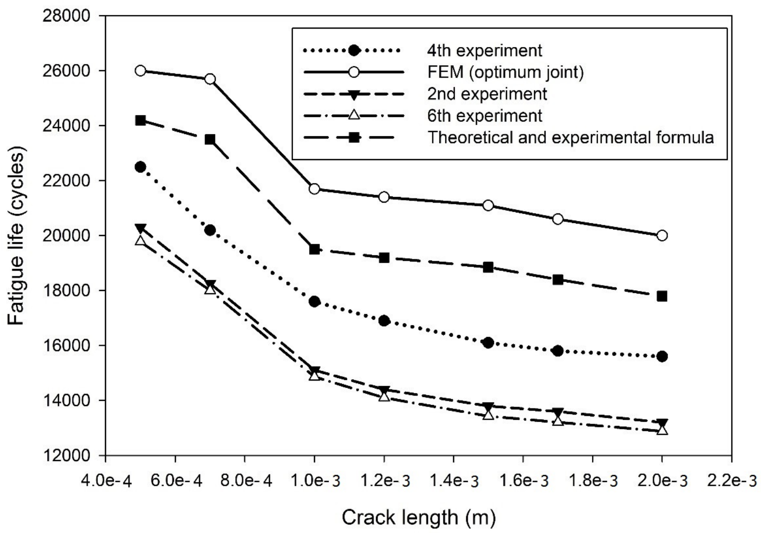

Fig. 9. A comparison between optimum fatigue life cycle and other experiments.

Another simulation process was accomplished for a number of experiments to achieve stress intensity factors. The crack geometry, loading and boundary conditions were the same as mentioned before. SIFs were calculated through finite element solution and fatigue life was estimated for all other experiments. As it is shown in Fig. 9, experiments of number

2 and 6 have lower fatigue life than optimum fatigue life because maximum residual stress field belongs to optimum joint. Moreover, fatigue life of the 4th experiment was higher than 2nd and 6th experiments because the levels of four factors in this experiment were closer to optimum joint than the other two experiments.

5. Validation

In order to validate the finite element simulations, another relationship is used for comparison. Eq. (10) shows the relationship between riveting squeeze force and the deformed head of the rivet. This relationship was derived experimentally by Rijck and co-workers. Figure 10 introduces the parameters which are used in such equation [20].

$$F_{sq} = \frac{1}{4}\pi D^2 K\left(2\ln(\frac{D}{D_0})\right)^n = \frac{1}{4}\pi D^2 K\left(\ln(\frac{H_0}{H})\right)^n \tag{10}$$

where K and n are strain hardening coefficient and strain hardening power, respectively. H_0 , H , D_0 and D are the rivet length out of the sheets before riveting process, rivet length out of the sheets after riveting process, rivet diameter before riveting, and rivet diameter after riveting (all these parameters are introduced schematically in Fig. 10), respectively.
As shown in Fig. 11, the results of Eq. (10) were compared with various forces (from 4000 N to 16000 N) as riveting squeeze force and the rivet tail dimensions for each simulation. Finally, FEM results and Rijck's experimental formula illustrated good accordance together.

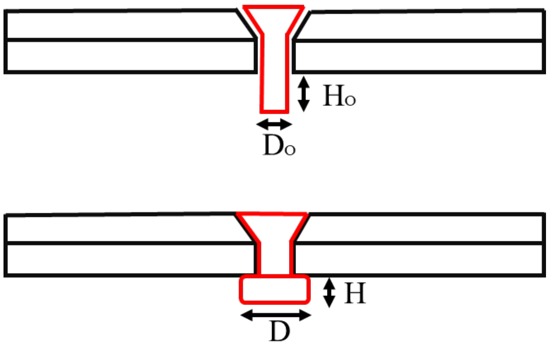

Fig. 10. Schematic of riveted joint and rivet tail parameters before and after riveting process.

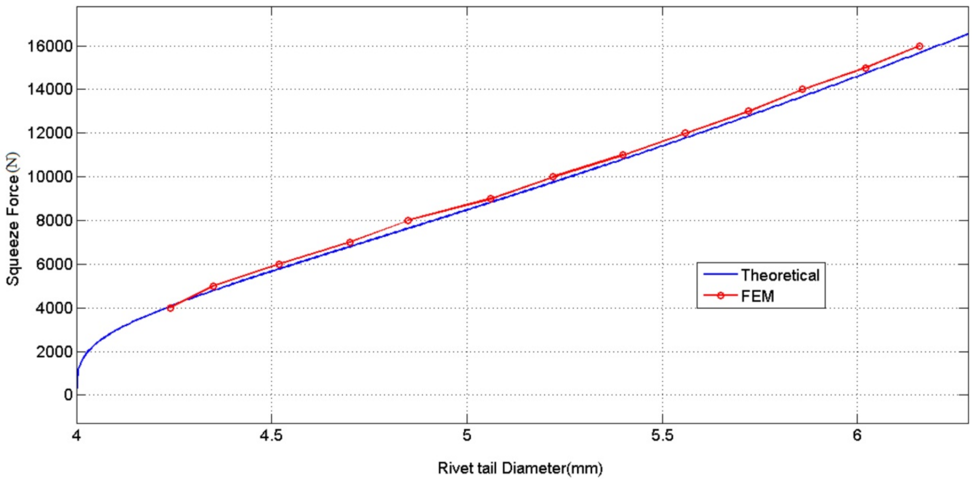

Fig. 11. Validation of finite element solution by Rijck's formula.

6. Conclusions

Effect of riveting process parameters is investigated by implementing finite element simulation and fatigue life of the joint is estimated using fracture mechanics approach and Paris-Erdogan rule. The following conclusions are obtained from the results:
1. When there are some restrictions in design, the knowledge about the most sensitive factor can be very useful to increase the residual stress field. Besides that, levels of each factor in which the maximum amount of residual stress field occurs, are determined and the optimum levels are achieved for riveting squeeze force, friction coefficient, sheet thickness

and clearance fit. Optimum levels for riveting squeeze force, friction coefficient, clearance fit and sheet thickness are in their 4th, 3rd, 4th and 2nd levels, respectively.
2. Residual stress field's sensitivity to variation is mostly dependent to riveting squeeze force and least dependent to clearance fit. In other words, a little change in riveting squeeze force causes much variation in residual stress field than the same change in other factors.
3. Although the increase in riveting squeeze force improves residual stress field, the increase in sheet thickness has negative effect on residual stress field.
4. The stress intensity factors and fatigue life for different crack lengths were obtained using finite element method and experimental formula. The comparison between these approaches revealed a good agreement. Therefore, it could be inferred that the finite element simulation of riveting process is capable to calculate stress intensity factors.
5. The optimum joint (riveting squeeze force of its 4th level: 16 kN, friction coefficient of its 3rd level: 0.6, clearance fit of its 4th level: 0.2mm, and sheet thickness of its 2nd level: 2.2mm) has a higher fatigue life than other simulations. Thus, it can be concluded that the maximum fatigue life is occurred in the optimum joint because it is optimized and designed based on maximizing residual stress field. Also, the more the levels of the four parameters close to their optimum condition, the more increase in fatigue life can be achieved. Hence, the optimum joint has the highest fatigue life among all other possible combinations in levels of the four factors and optimization procedure has increased fatigue life.
6. The relationship between Rivet head and riveting squeeze force is calculated through both its experimental formula and the finite element method in order to validate numerical procedure and a very good agreement is found between these two solutions.

Conflict of Interest

The authors declared no potential conflicts of interest with respect to the research, authorship and publication of this article.

Funding

The authors received no financial support for the research, authorship and publication of this article.

References

[1] Cheraghi, S.H., Effect of variations in the riveting process on the quality of riveted joints, *International Journal of Advanced Manufacturing Technology*, 39 (2008) 1144-1155.
[2] Iyer K., Rubin C.A., Hahn G.T., Three-dimensional analysis of single rivet row lap joints-part I: Elastic response, *Recent Adv Solids Struct*, 398 (1999) 23-39.
[3] Iyer K., Rubin C.A., Hahn G.T., Three-dimensional analysis of single rivet row lap joints-part I: Elastic-Plastic response, *Recent Adv Solids Struct*, 398 (1999) 41-57.
[4] Szolwinski M.P., Farris T.N., Linking riveting process parameters to the fatigue performance of riveted aircraft structures, *Journal of Aircraft*, 37(1) (2000) 130-137.
[5] Moreira P.M.G.P., de Matos P.F.P., Pinho S.T., Pastrama D., Camanho P.P., de Castro P.M.S.T., The residual stress intensity factors for cold-worked cracked holes: A technical note, *Fatigue and Fracture of Engineering Materials and Structures,* 27(9) (2004) 879-886.
[6] Rans C., Straznicky .PV., Riveting process induced residual stresses around solid rivets in mechanical joints, *Journal of Aicraft*, 44(1) (2007) 323-329.
[7] Kaifu Z., Hui C., Yuan L., Riveting process modeling and simulating for deformation analysis for aircraft's thin-walled sheet-metal parts, *Chinese Journal of Aeronautics*, 24 (2011) 369-377.
[8] Kafie-Martinez J., Keating P.B., Finite element modeling for clamping stresses developed in hot-driven steel structural riveted connections, *World Academy of Science, Engineering and Technology, International Journal of Civil, Environmental, Structural, Construction and Architectural Engineering*, 11(5) (2017) 634-639.
[9] Kafie-Martinez J., Keating P.B., Chakra-Varthy P., Correia J., de Jesus A., Stress distributions and crack growth in riveted lap joints fastening thick steel plates, *Engineering Failure Analysis*, 91 (2018) 370-381.
[10] Frost N.E., Marsh K.J., Pook L.P., *Metal fatigue*. Oxford University Press, London, 1974.
[11] Muller R.P.G., An experimental and analytical investigation on the fatigue behavior of fuselage riveted lap joints. PhD Thesis, Delft University of Technology, Delft, The Netherlands, 1995.
[12] Fung C.P., Smart J., Riveted single lap joints. Part 1: Fatigue life prediction, *Proceedings of the institution of mechanical engineers, part G (Journal of Aerospace Engineering)*, 211(1) (1997) 13-27.
[13] Fung C.P., Smart J., Riveted single lap joints. Part 2: A numerical parametric study, *Proceedings of the institution of mechanical engineers, part G (Journal of Aerospace Engineering)*, 211(2) (1997) 123-128.
[14] Deng X., Hutchinson J.W., The clamping stress in a cold driven rivet, *International Journal of Mechanical Sciences*, 40(7) (1998) 683-694.
[15] Trego A., Cope D., Evaluation of damage tolerance analysis tools for lap joints, *AIAA Journal*, 39(12) (2001) 2250-2254.
[16] Urban M.R., Analysis of the fatigue life of riveted sheet metal helicopter airframe joints, *International Journal of*

Fatigue, 25 (2003) 1013-1026.
[17] Skorupa M., Skorupa A., Machniewicz T., Korbel A., Effect of production variables on the fatigue behaviour of riveted lap joints, *International Journal of Fatigue*, 32 (2010) 996-1003.
[18] Pavan Kumar D.V.T.G., Sathiya Naarayan S., Kalyana Sundaram S., Chandra S., Further numerical and experimental failure studies on single and multi-row riveted lap joints, *Engineering Failure Analysis*, 20 (2012) 9-24.
[19] Moslemi H., Farhangdoost Kh., Zamani P., Fatigue life evaluation of single and two riveted coach peel joints using strain-life criteria, *AUT Journal of Mechanical Engineering*, 2019, DOI: 10.22060/AJME.2019.14541.5731.
[20] Rijck J.J.M., Homan J.J., Schijve J., Benedictus R., The driven rivet head dimensions as an indication of the fatigue performance of aircraft lap joints, *International Journal of Fatigue*, 29 (2007) 2208-2218.
[21] Zamani P., Jaamialahmadi A., Shariati M., Ductile failure and safety optimization of gas pipeline, *Journal of Solid Mechanics*, 8 (2016) 744-755.
[22] Yoon H.K., Lee S.P., Min B.H., Kim S.W., Katoh Y., Kohyama A., Fatigue life and fatigue crack propagation behavior of JLF-1 steel, *Fusion Engineering and Design*, 61 (20020 677-682.
[23] Paris P.C., Erdogan F., A critical analysis of crack propagation laws, *Transactions ASME Journal of Basic Engineering*, 85 (1963) 528-534.
[24] Peterson R.E., *Stress concentration design factors*, John Wiley & Sons, New York, 1953.
[25] Beuth J.L., Hutchinson J.W., Fracture analysis of multi-site cracking in fuselage lap joints, *Computational Mechanics*, 13 (1994) 315-331.
[26] Rijck J.J.M., Fawaz S.A., Schijve J., Benedictus R., Homan J.J., Stress analyses of mechanically fastened joints in aircraft fuselages, *24th ICAF Symposium*, Naples, 2007.
[27] Jiang H., Li G., Zhang X., Cui J., Fatigue and failure mechanism in carbon fiber reinforced plastics/ aluminum alloy single lap joint produced by electromagnetic riveting technique, *Composites Science and Technology*, 152 (2017) 1-10.
[28] Mohajerzadeh S., Farhangdoost Kh., Zamani P., Kolasangiani K., Experimental investigation on fatigue evaluation of orthopaedic locking compression plate, *International Journal of Advanced Design and Manufacturing Technology*, 11(4) (2018) 47-52.

ORCID iD

Pedram Zamani https://orcid.org/0000-0003-4560-9680
Khalil Farhangdoost https://orcid.org/0000-0001-5463-6766